Lithuanian Journal of Physics
Vol. **65**, No. 4, pp. 236–247 (2025)
ISSN 1648-8504 eISSN 2424-3647
DOI: https://doi.org/10.3952/physics.2025.65.4.6

SURFACE ANALYSIS OF CARBON ALLOTROPES

S. Kaciulis

Institute for the Study of Nanostructured Materials, ISMN – CNR, PO Box 10, 00015 Monterotondo Scalo (RM), Italy
Email: saulius.kaciulis@cnr.it

Received 30 October 2025; accepted 3 December 2025

The spectroscopy of carbon is very important in surface analysis of solids, because its content indicates the grade of surface contamination. Adventitious carbon from air ambient is practically present on any solid material and the C 1s photoelectron spectrum is often used as a reference for the scale calibration of binding energy. Moreover, during the last two decades, new 2D carbon materials have been developed and intensively investigated: graphene, fullerenes, nanotubes and nanowalls, quantum dots, etc. Also, the growing applications of amorphous carbon (a-C), e.g. diamond-like carbon (DLC), carbon quantum dots (CQDs), etc., require the characterization of these materials. This short overview is dedicated to the analysis of new carbon-based materials by widely used surface-sensitive techniques: X-ray photoelectron spectroscopy (XPS) and Auger electron spectroscopy (AES). The combination of XPS and AES techniques permits one to investigate the electron hybridization in carbon materials, i.e. to determine the ratio of sp^2/sp^3 configurations, which defines their main mechanical, electrical and optical properties. In addition, it was demonstrated that the same experimental approach could be successfully used for the investigation of bulk composite materials containing 2D carbon, e.g. graphene or nanotubes.

Keywords: carbon electron hybridization, 2D carbon, XPS, AES

1. Introduction

Carbon is a chemical element with a low atomic number of 6 and the electron configuration for a neutral carbon atom is $1s^2 2s^2 2p^2$. Therefore, it has only six electrons: two in the first orbital 1s, two in the second orbital 2s and the last two in the 2p orbitals. For this reason, in surface analysis it is possible to excite only two detectable signals: the photoemission line of C 1s and the Auger line C KLL, which is really a convolution of C KVV transitions. Due to the surface contamination, both spectra of C 1s and C KVV are observed almost on any sample investigated by X-ray photoelectron spectroscopy (XPS) or Auger electron spectroscopy (AES). Very often, the position of C 1s peak is used for the calibration of binding energy (BE) scale in XPS, whereas from the shape of C KVV spectra it is possible to extract the information on the electron hybridization states of carbon, because it contains the convolution of 1s-2pp-2pp and 1s-2ps-2pp transitions. Carbon electrons can be hybridized in fourfold sp^3 (diamond), threefold sp^2 (graphite) and even in linear sp^1 symmetries [1, 2]. This information is very important for still increasing research dedicated to the investigation and application of new 2D carbon materials, such as graphene, fullerenes, nanotubes and nanowalls, quantum dots, etc. Even in amorphous carbon (a-C) and diamond-like carbon (DLC), where both types of sp^2 and sp^3 carbon bonds are present: it is their ratio that determines the mechanical, electrical and optical properties of these materials.

Numerous experimental techniques can be used for the determination of sp^2 and sp^3 bonds in carbon materials: neutron diffraction, nuclear magnetic resonance, electron energy loss spectroscopy (EELS), Raman spectroscopy, transmission electron microscopy (TEM), Fourier transform infrared spectroscopy, etc. Nevertheless, most of them are not surface-sensitive and can modify the sample structure, others (e.g. surface-enhanced Raman) can yield only indirect information on the sp^2/sp^3 ratio. Therefore, the most suitable techniques for this purpose are the surface-sensitive and non-destructive electron spectroscopies: X-ray photoelectron spectroscopy (XPS), Auger electron spectroscopy (AES) and EELS.

XPS is a widely accepted surface analysis technique [3, 4] for the investigation of carbon spectra C 1s and C KVV. In the case of C KVV spectra, it is more correct to describe it as XAES (X-ray induced AES). However, when only photoemission spectra C 1s are analysed, the final results are based on the peak fitting, which strongly depends on its parameters: peak values in binding energy (BE), shape and full width at half-maximum (FWHM). These parameters depend on initial assumptions, which can easily lead to ambiguous conclusions on carbon allotropes. The most important assumptions are the positions of synthetic peaks of diamond and graphite, i.e. two pure cases of carbon sp^3 and sp^2 hybridization.

In the literature, the experimental BE value of graphite is more accurate, moving only in a range of 284.3–284.7 eV [4–10], and that is easily explained by the absence of sample charging in the semimetal and correct calibration of BE scale by using the Fermi edge at BE = 0 eV. Of course, for the correct C 1s peak fitting, it is necessary to use an asymmetric Doniach–Šunjic function [9, 11] characteristic of metals and semimetals. In contrast to graphite, a very large uncertainty exists for diamond: its BE values are scattered between about 284 eV [12–15] to about 286 eV [13, 16, 17]. This uncertainty of the peak position is due to the sample charging caused by electrical insulation of diamond, especially if it is an undoped one. Anyway, the most important for the correct peak fitting are not the absolute BE values, but the chemical shift between synthetic C 1s peaks of graphite and diamond. The experimental results and theoretical calculations of this shift are changing from negligible values of –0.2 eV [12, 18, 5, 7, 15, 19, 20] to relatively high ones, between 0.7–1.5 eV [16, 21, 22, 6, 17, 23–26]. This scattering can be explained by the sample charging or by the shift between BE values for the diamond surface and bulk [5]. In the majority of experimental XPS studies of DLC films, the shift values between sp^2 and sp^3 states are at about 0.5–1 eV [4, 6, 11, 16, 17, 26–41], whereas in some articles, this shift is considered to be very small and the separation of both peaks is not used at all [18, 20, 42, 43]. Moreover, for any BE values in C 1s peak fitting, it is necessary to remember that on the surface of a-C or DLC films an aliphatic carbon is always present, characterized by BE = 285.0 eV [4, 13, 44]. In conclusion, the calculation of sp^2/sp^3 ratio, based only on C 1s peak fitting, is not a reliable procedure without any supporting data of other measurements.

Also, the direct photoemission investigation of convolved 2ps and 2pp states in the carbon valence band (VB) can be implemented by means of XPS or ultraviolet photoelectron spectroscopy (UPS) [7, 11, 12, 15, 18, 20, 29, 33, 45–47]. Anyway, it is quite difficult to quantify the sp^2 and sp^3 configurations only from the broad features in VB spectra. In addition, the photoemission signals in these spectra are low in comparison with core level photoemission and AES.

In AES and XAES techniques, the C KVV spectrum, composed of 1s-2pp-2pp and 1s-2ps-2pp transitions, is acquired and analysed. This convolution results in a wide signal with a complex structure, which also contains the information about the electronic structure of the carbon valence band (2s and 2p orbitals), i.e. the hybridization of carbon electrons [6, 19, 20, 45, 48–50]. It is known that the detailed analysis of C KVV spectra is easier in the first derivative form, which is better representing a fingerprint of carbon electronic hybridization states [6, 49]. A simplified method of this analysis is based on the measurement of peak-to-peak width (D parameter) and applying its linear calibration for the whole hybridization range from diamond to graphite [33, 42]. This approach has been successfully used in numerous studies of sp^2/sp^3 ratio in a-C and DLC films [26–28, 40, 41, 43, 51], multiwall carbon nanotubes [25, 32, 52] and nanodiamonds [24, 25, 48, 53]. Later, the method of principal component analysis has been developed, which enables the numerical identification of C 1s, C KVV and energy loss signals and the accurate determination of sp^2/sp^3 ratio [25, 54, 55]. However, it is based on the experimental statistics of voluminous spectroscopic data, therefore, not suitable for the rapid characterization of carbon materials.

EELS is one more spectroscopic technique, which can be used for the investigation of carbon materials. There are two characteristic features of carbon electronic configuration in EELS spectra: the π-related peak at the loss energy of 5–6 eV and the $\sigma+\pi$ plasmon at about 23–30 eV [21]. This experimental method is reliable for pure allotropes (diamond or graphite) and amorphous

carbon [12, 18, 56–58], but its sensitivity becomes too low in the case of low ratios of sp^2/sp^3 [11, 21, 22].

In this paper, we present a brief overview of recent experimental studies on carbon materials carried out in our laboratory at ISMN-CNR by using combined XPS and AES techniques. Many different materials, starting from the reference samples (diamond, graphite and graphene) and continuing with a-C, DLC and 2D carbon (graphene and its oxide, fullerenes, nanotubes and nanowalls, quantum dots), have been investigated for the identification of surface chemical composition, including carbon allotropes.

2. Experimental techniques

XPS and AES measurements have been carried out by using two electron spectrometers: an Escalab MkII (*VG Scientific Ltd*., UK) and an Escalab 250 Xi (*Thermo Fisher Scientific* Ltd., UK). The first one was equipped with a non-monochromatic Al Kα X-ray source ($h\upsilon$ = 1486.6 eV), a LEG200 electron gun and a five-channeltron detection system. The second one was equipped with a monochromatic Al Kα X-ray source, an EX06 Ar^+ ion gun for surface cleaning, a combined system of electrostatic/electromagnetic input lens and a six-channeltron detector. In both spectrometers, the analysed sample area was about 1 mm in diameter and the photoelectron spectra were collected at constant pass energy of 20 or 40 eV, whereas Auger spectra excited by X-ray photons of electron beam were acquired at 100 eV pass energy in order to increase the signal-to-noise ratio. During the measurements, the base pressure in the analysis chamber was about 1×10^{-8} Pa. The binding energy (BE) scale was calibrated by positioning the reference peak of Au $4f_{7/2}$ from the sample mask to BE = 84.0 eV. The accuracy of the measured BE was ±0.1 eV.

All spectroscopic data were collected and processed by the Avantage v.5.9 software (*Thermo Fisher Scientific Ltd*., UK), using a peak-fitting routine with the Shirley background and symmetrical Gaussian–Lorentzian mixture of 70 and 30%, respectively. Experimental C KVV spectra were smoothed at least for 11 times by the moving average routine with a width of 1.2 eV. Afterwards, those spectra were differentiated by using a width of 7 data points for the determination of D parameter [60].

Some selected samples have been investigated by high-resolution XPS and XAES measurements performed at the ESCA microscopy beamline of *Elettra* synchrotron in Trieste, Italy. All the spectra of C 1s and C KVV regions were acquired with 0.2 eV resolution in energy by using a 700 eV photon beam. The energy scale was calibrated by using the Fermi edge of the VB spectra. More experimental details on this beamline have been reported elsewhere [61].

3. Results and discussion

In the detailed XPS study of numerous reference samples of elemental carbon [60, 62], conducted without any BE scale correction for sample charging, it was concluded that the chemical shift of C 1s peak between sp^2 and sp^3 hybridization (graphite and diamond) is negligible (see Fig. 1) and the peak fitting procedure can be ambiguous, i.e. it depends on the initial positions of sp^2 and sp^3 components, especially in the case of a-C or DLC samples with an unknown composition and some contribution of aliphatic carbon [4, 62]. Therefore, the previous suppositions [5, 7, 12, 15, 18–20] of impossibility to identify the carbon

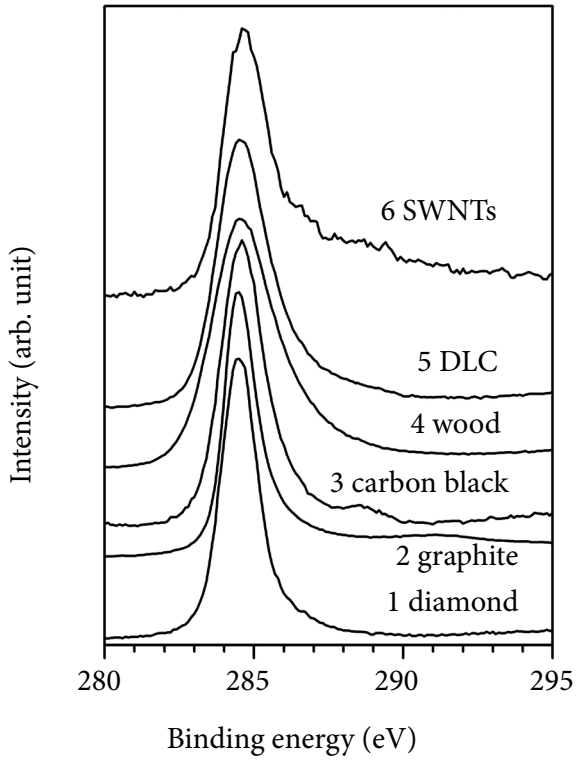

Fig. 1. Comparison of C 1s spectra of different carbon samples [62].

hybridization only from the C 1s peak fitting were fully confirmed.

In the same study, also the energy losses of C 1s photoelectrons were carefully analysed. Characteristic losses in the freshly cleaved sample of highly oriented pyrolytic graphite (HOPG) were identified as $\pi - \pi^{\star}$ excitation at 6.0 eV and the plasmons of s + p valence electrons at 26.1 and 34.9 eV. In the monocrystalline diamond, three typical losses at 15.8, 24.2 and 34.4 eV were observed, as in Ref. [63]. Of course, these losses enable one to identify pure diamond and graphite, but their overlapping hinders the determination of sp^2/sp^3 ratio in other carbon materials.

The correct assessment of sp^2/sp^3 ratio in other carbon materials (a-C, a-C:H, DLC, etc.) is the acquisition of C KVV spectra (by using XAES or AES) and the determination of their width, i.e. the D parameter, which is illustrated in Fig. 2 [60]. As it is linearly proportional to the sp^2/sp^3 ratio, the determination of carbon hybridization becomes quite simple and accurate. The results obtained for a series of various carbon allotropes are displayed in Fig. 3 [62]. The plot linearity between the samples of pure diamond and graphite is confirmed by the experimental point #6 (sp^2 = 68%) obtained for a certified sample of a-C with sp^2 = 66%. When the same method was applied for a series of DLC films, produced by plasma enhanced chemical vapour deposition (PECVD), it revealed the influence of deposition parameters on the material composition [64].

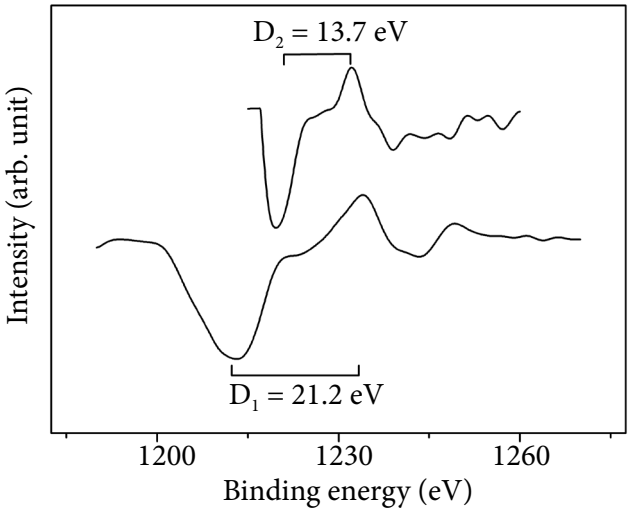

Fig. 2. Derivative of C KLL spectra for graphite (D_1) and diamond (D_2). Reprinted from Ref. [60].

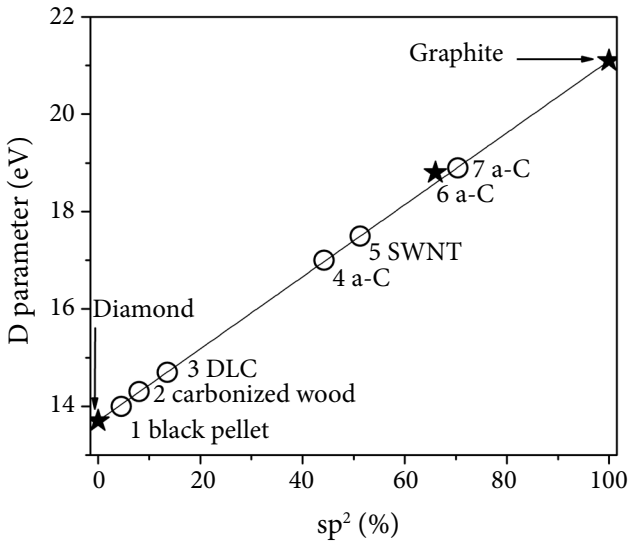

Fig. 3. D parameter versus percentage of sp^2 [62].

Afterwards, a particular effect was observed in the C KVV spectra of 2D carbon materials. Starting with graphene, which is a relatively simple material, composed of a single layer of carbon in a hexagonal (i.e. graphitic) structure and has a high electron mobility like semimetals or zero gap semiconductors [65], and going on with other 2D carbons (nanotubes, quantum dots, etc.), we shall see that the same phenomenon is present in all these materials. Previously, numerous analytical methods have been applied for graphene characterization, including Raman spectroscopy, atomic force microscopy (AFM), low energy electron diffraction (LEED), XPS and AES [23, 66–77]. The usage of AES and Raman have been the most informative ones, because these techniques can identify the graphene structure from characteristic signals [66–70, 73–75], determine the number of graphene layers [66, 68, 70, 73, 74] and obtain the chemical maps of graphene on conductive substrates [67, 73].

Our first study of graphene [78] was focused on the shape of the Auger C KVV signal and the related D parameter, beginning with experiments using the excitation by electron beam (AES) and X-ray photons (XAES) for certified commercial samples, deposited by CVD on Cu and SiO_2 substrates, and comparing them with the reference samples of HOPG and monocrystalline diamond. XPS C 1s spectra of both samples, besides the main asymmetric graphitic peak at BE = 284.6 eV, contained two peaks of low intensity: C–O bonds and surface defects at BE = 286.0 eV and carboxylic O–C=O

bonds at BE ≈ 288 eV [70, 72, 78–80]. The peak areas of secondary peaks did not exceed 11 and 5%, respectively. From the area ratio of C 1s and substrate peaks (Cu 2p or Si 2p), an average thickness of graphene films was calculated: about 0.6 and 1 nm on Cu and Si, respectively. Obviously, those values were averaged over the area of XPS analysis (diameter ≈ 1 mm) and can be overestimated due to the influence of surface contaminants and graphene ripples.

A big surprise was the C KVV spectra of graphene (see Fig. 4), acquired by using XAES. Those spectra were very similar to the C KVV spectrum of pure diamond [60, 62], especially if we calculate the values of D parameter. In contrast, the AES spectra of graphene were identical to the ones of graphite (HOPG sample), as it was reported in the literature [66, 73, 74]. As it was expected, the D values for graphite (D = 21.2 and 21.0 eV) and diamond (13.7 and 14.2 eV) were almost independent of the excitation source, whereas for graphene, they were diamond-like in XAES (D = 14–15 eV) and graphitic in AES (D = 20.4 eV). When the sample of graphene on Cu was heated to 400°C, the D parameter in XAES was slightly increased to D = 15.2 eV and decreased to the value of pure diamond (D = 13.5 eV) when the sample was cooled by liquid nitrogen.

As the ideal graphene has pure sp^2 carbon hybridization, it seems logical to expect its C KVV spectrum to be identical to that of graphite. However, this spectrum is arising from the convolution of π and π-σ holes in VB, thus in 2D carbon, it can be influenced by the strong screening near to the Fermi level [81, 82]. Due to this effect, the C KVV spectra of 2D carbon can be different from graphite, as it was indicated by theoretical calculations [83]. In addition, the similar changes have been noticed previously [83, 84] in the experimental C KVV spectra of single wall carbon nanotubes (SWCNTs), which are the wrapped sheets of graphene. The diamond-like value of D parameter in XAES can be very useful for the experimental identification of graphene, and later this method has been also used for investigations of graphene quantum dots (GQDs) and graphene oxide (GO) reduction.

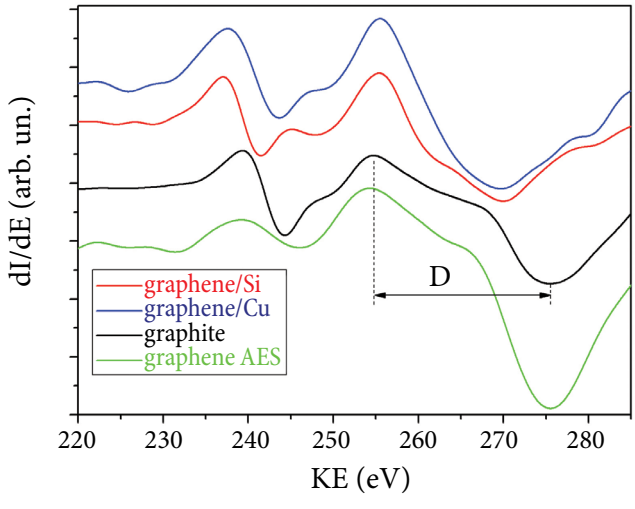

Fig. 4. First derivative of the C KVV spectra of graphene and graphite [78].

A different shape of the AES spectra and graphitic values of the D parameter observed for graphene can be explained by a high intensity of the electron beam, which creates a high density of scattered electrons on the sample surface. A high density of free electrons can cancel the 2D effect in the proximity of the Fermi level of graphene and result in the graphitic C KVV spectrum. This supposition has been confirmed by the XAES spectra of graphene irradiated with low energy electrons (50–120 eV) from the flood gun [78]. Under the flux of electrons, the width of the C KVV spectrum was increasing together with electron energy and the D parameter went up to 15.5 eV, i.e. it was shifted towards the graphitic value.

Obviously, it is possible to expect some influence of the screening near to the Fermi level to the shape of graphene VB spectra. The comparison of the VB spectra, acquired for graphene and graphite (HOPG) by UPS using the He II source of 40.8 eV [78], confirmed the absence of occupied states in graphene near to the Fermi edge (up to about BE = 4 eV), whereas in graphite, those states were present already at BE = 0 eV (see Fig. 5). This difference between the VB structure of graphite and 2D carbon was indicated also in other studies [83, 84]. It should be noted that very similar effects were also observed in the spectroscopic comparison of monocrystalline and hydrogenated diamond samples [78]. While the signal in the VB spectrum of pure diamond started only from about BE = 2 eV, in hydrogenated ones, it was increasing already from the Fermi level. The same effect of occupied states near the Fermi edge was also observed in the C KVV spectra of hydrogenated

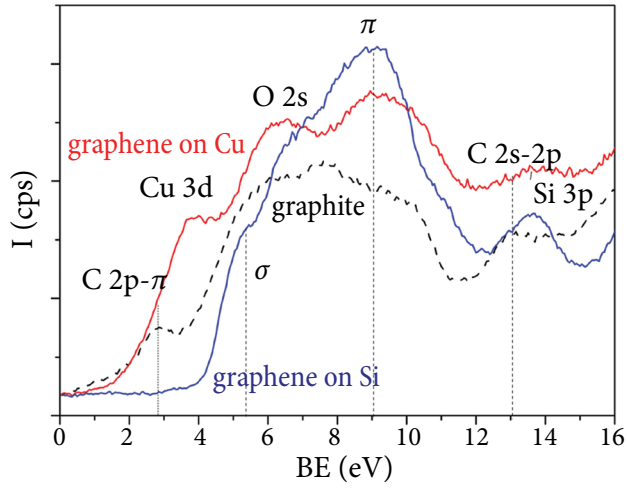

Fig. 5. Comparison of valence band spectra: graphite and graphene on different substrates [78].

diamonds, where the D parameter was increased up to 20.2 eV, i.e. almost to the graphitic value.

The experimental method of D parameter (comparison of its values in XAES and AES spectra) was successfully used for graphene identification in the samples grown by CVD on polycrystalline Cu, Ni and NiCu substrates [85, 86]. The same technique was used also for the study of thermal GO reduction [87], where by the combined analysis of D parameter and C 1s spectra, the successful reduction to graphene was demonstrated after annealing in the ultrahigh vacuum (UHV) at 600°C, which is illustrated in Fig. 6. The oxidation of pure graphite

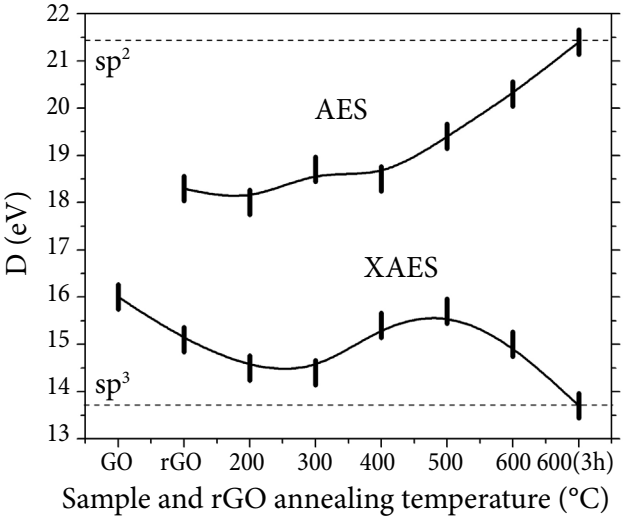

Fig. 6. D parameter of the reduced GO sample vs annealing temperature. AES is Auger electron spectroscopy; XAES is X-ray induced AES. Reprinted from Ref. [87].

powder and the results of the thermal and hydrothermal reduction of produced GO films were later studied by XPS and AES in Ref. [89]. The obtained results demonstrated that the reduction occurred on both the edges and the basal plane of each particle when the oxygen functional groups were partly removed. Moreover, the values of D parameter were significantly decreased after reduction, indicating that the graphene structure was not fully achieved, but a more ordered graphene-like structure was created in the films.

When the same approach of united XPS and AES techniques has been applied for the detailed investigation of chemically unfolded buckminsterfullerene, the obtained results manifested the dominant presence of graphene-like carbon in the produced nanoplatelets of GQDs [89, 90]. Moreover, the XPS analysis also permitted the identification of the GQDs border interaction with dissolved in water metal ions (Hg, Cd, Pb, Cu, Ni and As) that were bonded via carboxylic groups.

An interesting phenomenon has been observed in the composites, i.e. in the bulk materials containing 2D carbon. It was discovered in two types of composites: matrix of natural rubber latex with graphene platelets and epoxy resin filled with micro-particles of Ag and graphene or carbon nanotubes [91]. In all those composites, the XAES values of D parameter were diamond-like (12–14 eV), whereas the AES values were completely graphitic (20–22 eV), i.e. the presence of graphene or SWCNTs was reliably identified and also verified by TEM images. Due to the segregation of 2D carbon on the surface of composites, even a very small content was sufficient for its recognition [91].

Afterwards, the same experimental method was applied for the characterization of different composite materials with 2D carbon: graphene-alumina heterostructured films [92], amorphous vinyl alcohol composites [93] and cementitious nanocomposites [94, 95], whereas a simplified characterization limited to the XPS study of carbon bonds (C 1s signal) and the chemical state of other constituent elements was employed for the composites with GO [96–98].

4. Conclusions

A new experimental method for the characterization of carbon materials, based on combined XPS

and AES analyses, was developed and tested by using the reference samples of graphite, diamond and graphene [60, 62, 78]. This method is based on the correct peak fitting of C 1s photoemission spectra and the determination of D parameter (i.e. sp^2/sp^3 ratio of carbon hybridization) from Auger spectra C KVV. Afterwards, it was successfully applied for the investigation of various carbon materials containing 2D carbon (graphene, SWCNTs, GQDs) and materials with intermediate carbon hybridization, e.g. a-C, DLC, GO and CQDs.

Acknowledgements

The author is sincerely grateful to Prof. Juras Požela, the supervisor of his PhD studies at the Semiconductor Physics Institute (Vilnius, Lithuania), who later indicated a promising research direction in surface science and supported the beginning of his scientific activities in this field. Also, many thanks for the fruitful collaboration to the colleagues at the Surface Analysis Laboratory of ISMN-CNR and in other Italian research institutions.

References

[1] J. Robertson, Mechanism of sp^3 bond formation in the growth of diamond-like carbon, Diamond Rel. Mater. **14**, 942–948 (2005).

[2] Y. Lifshitz, Diamond-like carbon – present status, Diamond Rel. Mater. **8**, 1659–1676 (1999).

[3] P.K. Chu and L. Li, Characterization of amorphous and nanocrystalline carbon films, Mater. Chem. Phys. **96**, 253–277 (2006).

[4] M. Walter, F. Mangolini, J. Brandon McClimon, R.W. Carpick, and M. Moseler, Origin of C(1s) binding energy shifts in amorphous carbon materials, Phys. Rev. Mater. **9**, 035601 (2025).

[5] J.F. Morar, F.J. Himpsel, G. Hollinger, J.L. Jordan, G. Hughes, and F.R. Mcfeely, C 1s excitation studies of diamond (111). I. Surface core levels, Phys. Rev. B **33**, 1340–1345 (1986).

[6] Y. Mizokawa, T. Miyasato, S. Nakamura, K.M. Geib, and C.W. Wilmsen, Comparison of the CKLL first-derivative Auger spectra from XPS and AES using diamond, graphite, SiC and diamond-like-carbon films, Surf. Sci. **182**, 431–438 (1987).

[7] F.R. McFeely, S.P. Kowalczyk, L. Ley, R.G. Cavell, R.A. Pollak, and D.A. Shirley, X-ray photoemission studies of diamond, graphite, and glassy carbon valence bands, Phys. Rev. B **9**, 5268–5278 (1974).

[8] P.A. Brühwiler, A.J. Maxwell, C. Puglia, A. Nilsson, S. Anderson, and N. Martensson, Pi-asterisk and sigma-asterisk excitons in C-1s absorption of graphite, Phys. Rev. Lett. **74**, 614–617 (1995).

[9] S. Lizzit, L. Petaccia, A. Goldoni, R. Larciprete, Ph. Hofmann, and G. Zampieri, C 1s photoemission spectrum in graphite(0001), Phys. Rev. B **76**, 153408 (2007).

[10] S.-S. Lin, Surface characterization of ion-beam modified graphite, Carbon **31**, 509–517 (1993).

[11] J. Diaz, G. Paolicelli, S. Ferrer, and F. Comin, Separation of the sp^3 and sp^2 components in the C1s photoemission spectra of amorphous carbon films, Phys. Rev. B **54**, 8064–8069 (1996).

[12] A. Cook, A.G. Fitzgerald, B.E. Storey, J.I.B. Wilson, P. John, M.G. Jubber, D. Milne, I. Drummond, J.A. Savage, and S. Haq, A microbeam analytical characterization of diamond films, Diamond Rel. Mater. **1**, 478–485 (1992).

[13] S. Ferro, M. Dal Colle, and A. De Battisti, Chemical surface characterization of electrochemically and thermally oxidized boron-doped diamond film electrodes, Carbon **43**, 1191–1203 (2005).

[14] K. Yamamoto, H. Yoshida, Surface modification of diamond using low-energy nitrogen ions, Diamond Rel. Mater. **13**, 736–739 (2004).

[15] P. Reinke and P. Oelhafen, The interaction of carbon with the diamond surface: An in-situ photoelectron spectroscopy investigation, Diamond Rel. Mater. **7**, 177–181 (1998).

[16] R. Haerle, E. Riedo, A. Pasquarello and A. Baldereschi, sp^2/sp^3 hybridization ratio in amorphous carbon from C 1s core-level shifts: X-ray photoelectron spectroscopy and first-principles calculation, Phys. Rev. B **65**, 045101 (2002).

[17] I.N. Shabanova, L.G. Makarova, N.S. Trebova, V.I. Ladyanov and R.M. Nikonova, X-ray photoelectron investigation of carbon nanostructures in iron matrix, J. Electron Spectr. Rel. Phenom. **156–158**, 191–194 (2007).

[18] Y. Fan, A.G. Fitzgerald, P. John, C.E. Troupe and J.I.B. Wilson, X-ray photoelectron spectroscopy studies of CVD diamond films, Surf. Interf. Anal. **34**, 703–707 (2002).

[19] L. Constant, C. Speisser, and F. Le Normand, HFCVD diamond growth on Cu(111). Evidence for carbon phase transformations by in situ AES and XPS, Surf. Sci. **387**, 28–43 (1997).

[20] G. Speranza and N. Laidani, Measurement of the relative abundance of sp^2 and sp^3 hybridised atoms in carbon based materials by XPS: a critical approach. Part I, Diamond Rel. Mater. **13**, 445–450 (2004).

[21] C. Godet, D. David, H. Sabbah, S. Ababou-Girard, and F. Solal, Bulk and surface plasmon excitations in amorphous carbon measured by core-level photoelectron spectroscopy, Appl. Surf. Sci. **255**, 6598–6606 (2009).

[22] J.T. Titantah and D. Lamoen, sp^3/sp^2 characterization of carbon materials from first-principles calculations: X-ray photoelectron versus high energy electron energy-loss spectroscopy techniques, Carbon **43**, 1311–1316 (2005).

[23] S. Rey and F. Le Normand, Surface transformations of carbon (graphene, graphite, diamond, carbide), deposited on polycrystalline nickel by hot filaments chemical vapour deposition, Thin Solid Films **519**, 4426–4428 (2011).

[24] F.Y. Xie, W.G. Xie, L. Gong, W.H. Zhang, S.H. Chen, Q.Z. Zhang, and J. Chen, Surface characterization on graphitization of nanodiamond powder annealed in nitrogen ambient, Surf. Interf. Anal. **42**, 1514–1518 (2010).

[25] B. Lesiak, J. Zemek, P. Jiricek, L. Stobinski, and A. Jozwik, The line shape analysis of electron spectroscopy spectra by the artificial intelligence methods for identification of C sp^2/sp^3 bonds, Phys. Stat. Sol. B **247**, 2838–2842 (2010).

[26] P. Mérel, M. Tabbal, M. Chaker, S. Moisa, and J. Margot, Direct evaluation of the sp^3 content in diamond-like-carbon films by XPS, Appl. Surf. Sci. **136**, 105–110 (1998).

[27] A. De Bonis, J.V. Rau, A. Santagata, and R. Teghil, Diamond-like carbon thin films produced by femtosecond pulsed laser deposition of fullerite, Surf. Coat. Technol. **205**, 3747–3753 (2011).

[28] J.V. Rau, R. Teghil, A. De Bonis, A. Generosi, B. Paci, R. Generosi, M. Fosca, D. Ferro, V.R. Albertini, and N.S. Chilingarov, Pulsed laser deposition of hard and superhard carbon thin films from C_{60} targets, Diamond Rel. Mater. **19**, 7–14 (2010).

[29] N. Paik, Raman and XPS studies of DLC films prepared by a magnetron sputter-type negative ion source, Surf. Coat. Technol. **200**, 2170–2174 (2005).

[30] J. Filik, P.W. May, S.R.J. Pearce, R.K. Wild, and K.R. Hallam, XPS and laser Raman analysis of hydrogenated amorphous carbon films, Diamond Rel. Mater. **12**, 974–978 (2003).

[31] J. Rao, K.J. Lawson, and J.R. Nicholls, The characterisation of e-beam evaporated and magnetron sputtered carbon films fabricated for atomic oxygen sensors, Surf. Coat. Technol. **197**, 154–160 (2005).

[32] L. Stobinski, B. Lesiak, L. Köver, J. Tóth, S. Biniak, G. Trykowski, and J. Judek, Multiwall carbon nanotubes purification and oxidation by nitric acid studied by the FTIR and electron spectroscopy methods, J. Alloys Compd. **501**, 77–84 (2010).

[33] J.C. Lascovich and S. Scaglione, Comparison among XAES, PELS and XPS techniques for evaluation of sp^2 percentage in a-C:H, Appl. Surf. Sci. **78**, 17–23 (1994).

[34] R. Paul, S. Hussain, S. Majumder, S. Varma, and A.K. Pal, Surface plasmon characteristics of nanocrystalline gold/DLC composite films prepared by plasma CVD technique, Mater. Sci. Eng. B **164**, 156–164 (2009).

[35] E. Balaur and A.G. Peele, Tunnelling through diamond-like carbon nanofilms deposited by electron-beam-induced deposition, Thin Solid Films **517**, 6520–6526 (2009).

[36] R.M. Dey, M. Pandey, D. Bhattacharyya, D.S. Patil, and S.K. Kulkarni, Diamond like carbon coatings deposited by microwave plasma CVD: XPS and ellipsometric studies, Bull. Mater. Sci. **30**, 541–546 (2007).

[37] H.-S. Zhang, J.L. Endrino, and A. Anders, Comparative surface and nano-tribological characteristics of nanocomposite diamond-like carbon

thin films doped by silver, Appl. Surf. Sci. **255**, 2551–2556 (2008).

[38] K. Yamamoto, Chemical bond analysis of amorphous carbon films, Vacuum **84**, 638–641 (2009).

[39] Ishpal, O.S. Panwar, M. Kumar, and S. Kumar, Effect of ambient gaseous environment on the properties of amorphous carbon thin films, Mater. Chem. Phys. **125**, 558–567 (2011).

[40] M. Jelinek, K. Smetana, T. Kocourek, B. Dvoránková, J. Zemek, J. Remsa, and T. Luxbacher, Biocompatibility and sp^3/sp^2 ratio of laser created DLC films, Mater. Sci. Eng. B **169**, 89-93 (2010).

[41] S.T. Jackson and R.G. Nuzzo, Determining hybridization differences for amorphous-carbon from the XPS C-1s envelope, Appl. Surf. Sci. **90**, 195–203 (1995).

[42] J.C. Lascovich, R. Giorgi, and S. Scaglione, Evaluation of the sp^2/sp^3 ratio in amorphous-carbon structure by XPS and XAES, Appl. Surf. Sci. **47**, 17–21 (1991).

[43] Q. Zhao, Y. Liu, C. Wang, and S. Wang, Bacterial adhesion on silicon-doped diamond-like carbon films, Diamond Rel. Mater. **16**, 1682–1687 (2007).

[44] G. Gusmano, G. Montesperelli, M. Rapone, G. Padeletti, A. Cusmà, S. Kaciulis, A. Mezzi, and R. Di Maggio, Zirconia primers for corrosion resistant coatings, Surf. Coat. Technol. **201**, 5822–5828 (2007).

[45] H.J. Steffen, Use of valence band Auger electron spectroscopy to study thin film growth: oxide and diamond-like carbon films, Thin Solid Films **253**, 269–276 (1994).

[46] S. Turgeon and R.W. Paynter, On the determination of carbon sp^2/sp^3 ratios in polystyrene–polyethylene copolymers by photoelectron spectroscopy, Thin Solid Films **394**, 44–48 (2001).

[47] L. Calliari, N. Laidani, and G. Speranza, X-ray and UV valence band photoemission of carbon films, Surf. Interf. Anal. **26**, 565–568 (1998).

[48] L. Constant and F. Le Normand, HF CVD diamond nucleation and growth on polycrystalline copper: A kinetic study, Thin Solid Films **516**, 691–695 (2008).

[49] Y. Mizokawa, T. Miyasato, S. Nakamura, K.M. Geib, and C.W. Wilmsen, The C-KLL 1st-derivative X-ray photoelectron-spectroscopy spectra as a fingerprint of the carbon state and the characterization of diamond-like carbon-films, J. Vac. Sci. Technol. A **5**, 2809–2813 (1987).

[50] K. Yamamoto, T. Watanabe, K. Wazumi, Y. Koga, S. Iijima, Carbon films deposited with mass-selected carbon ion beams under substrate heating, Surf. Coat. Technol. **169**, 328–331 (2003).

[51] I. Montero, L. Galan, A. Laurent, J. Perriere, and J. Spousta, X-ray photoelectron spectroscopy and X-ray-excited Auger electron spectroscopy studies of the initial deposition of hydrogenated amorphous carbon, Thin Solid Films **228**, 72–75 (1993).

[52] L. Stobinski, B. Lesiak, J. Zemek, P. Jiricek, S. Biniak, and G. Trykowski, Studies of oxidized carbon nanotubes in temperature range RT–630°C by the infrared and electron spectroscopies, J. Alloys Compd. **505**, 379–384 (2010).

[53] X. Liu, F. Klauser, N. Memmel, E. Bertel, I. Pichler, M. Knupfer, A. Kromka, and D. Steinmüller-Nethl, Spectroscopic studies of nanocrystalline diamond materials, Diamond Rel. Mater. **16**, 1463–1470 (2007).

[54] B. Lesiak, J. Zemek, J. Houdkova, P. Jiricek, and A. Jozwik, XPS and XAES of polyethylenes aided by line shape analysis: The effect of electron irradiation, Polymer Degr. Stabil. **94**, 1714–1721 (2009).

[55] B. Lesiak, J. Zemek, J. Houdkova, A. Kromka, and A. Jozwik, Electron spectra line shape analysis of highly oriented pyrolytic graphite and nanocrystalline diamond, Anal. Sci. **26**, 217–222 (2010).

[56] J. A. Leiro, M.H. Heinonen, T. Laiho, and I.G. Batirev, Core-level XPS spectra of fullerene, highly oriented pyrolytic graphite, and glassy carbon, J. Electron Spectr. Rel. Phenom. **128**, 205–213 (2003).

[57] V.N. Vasilets, A. Hirose, Q. Yang, A. Singh, R. Sammynaiken, M. Foursa, and Y.M. Shulga, Characterization of doped diamond-like carbon films deposited by hot wire plasma sputtering of graphite, Appl. Phys. A **79**, 2079–2084 (2004).

[58] K. Yamamoto, T. Watanabe, K. Wazumi, F. Kokai, Y. Koga, and S. Fujiwara, The sp^3 bond fraction in carbon films prepared by mass-separated ion beam deposition, Diamond Rel. Mater. **10**, 895–899 (2001).

[59] K. Yamamoto, T. Watanabe, K. Wazumi, Y. Koga, and S. Iijima, Effect of substrate temperature on the structure and chemical bonds of carbon films deposited with a mass-separated carbon ion beam, Diamond Rel. Mater. **12**, 2088–2092 (2003).

[60] A. Mezzi and S. Kaciulis, Surface investigation of carbon films: from diamond to graphite, Surf. Interface Anal. **42**, 1082–1084 (2010).

[61] S. Gunther, B. Kaulich, L. Gregoratti, and M. Kiskinova, Photoelectron microscopy and applications in surface and materials science, Prog. Surf. Sci. **70**, 187–260 (2002).

[62] S. Kaciulis, Spectroscopy of carbon: from diamond to nitride films, Surf. Interface Anal. **44**, 1155–1161 (2012).

[63] D. Marton, K.Y. Boyd, A.H. Al-Bayati, S.S. Todorov, and J.W. Rabalais, Carbon nitride deposited using energetic species: A two-phase system, Phys. Rev. Lett. **73**, 118–121 (1994).

[64] D. Caschera, P. Cossari, F. Federici, S. Kaciulis, A. Mezzi, G. Padeletti, and D.M. Trucchi, Influence of PECVD parameters on the properties of diamond-like carbon films, Thin Solid Films **519**, 4087–4091 (2011).

[65] C.N.R. Rao, A.K. Sood, R. Voggu, and K.S. Subrahmanyam, Some novel attributes of graphene, J. Phys. Chem. Lett. **1**, 572–580 (2010).

[66] M. Xu, D. Fujita, J. Gao, and N. Haganata, Auger electron spectroscopy: A rational method for determining thickness of graphene films, ACS Nano **4**, 2937–2945 (2010).

[67] J.H. Gao, N. Ishida, I. Scott, and D. Fujita, Controllable growth of single-layer graphene on a Pd(111) substrate, Carbon **50**, 1674–1680 (2012).

[68] J.H. Gao, K. Sagisaka, M. Kitahara, M.S. Xu, S. Miyamoto, and D. Fujita, Graphene growth on a Pt(111) substrate by surface segregation and precipitation, Nanotechnology **23**, 055704 (2012).

[69] A.C. Ferrari, J.C. Meyer, V. Scardaci, C. Casiraghi, M. Lazzeri, F. Mauri, S. Piscanec, D. Jiang, K.S. Novoselov, S. Roth, and A.K. Geimet, Raman spectrum of graphene and graphene layers, Phys. Rev. Lett. **97**, 187401 (2006).

[70] N. Sharma, D. Oh, H. Abernathy, M. Liu, P.N. First, and T.M. Orlando, Signatures of epitaxial graphene grown on Si-terminated 6H-SiC (0001), Surf. Sci. **604**, 84–88 (2010).

[71] E.Y. Polyakova, K.T. Rim, D. Eom, K. Douglass, R.L. Opila, T.F. Heinz, A.V. Teplyakov, and G.W. Flynn, Scanning tunneling microscopy and X-ray photoelectron spectroscopy studies of graphene films prepared by sonication-assisted dispersion, ACS Nano **5**, 6102–6108 (2011).

[72] D. Yang, A. Velamakanni, G. Bozoklu, S. Park, M. Stoller, R.D. Piner, S. Stankovich, I. Jung, D.A. Field, C.A. Ventrice, and R.S. Ruoff, Chemical analysis of graphene oxide films after heat and chemical treatments by X-ray photoelectron and micro-Raman spectroscopy, Carbon **47**, 145–152 (2009).

[73] M. Xu, D. Fujita, J. Gao, and N. Haganata, Monitoring electron-beam irradiation effects on graphenes by temporal Auger electron spectroscopy, Nanotechnology **21**, 265705 (2010).

[74] J. Lahiri, T. Miller, L. Adamska, I.I. Oleynik, and M. Batzill, Graphene growth on Ni(111) by transformation of a surface carbide, Nano Lett. **11**, 518–522 (2011).

[75] J. Lahiri and M. Batzill, Graphene destruction by metal-carbide formation: An approach for patterning of metal-supported graphene, Appl. Phys. Lett. **97**, 023102 (2010).

[76] R. Larciprete, S. Ulstrup, P. Lacovig, M. Dalmiglio, M. Bianchi, F. Mazzola, L. Hornekaer, F. Orlando, A. Baraldi, P. Hofmann, and S. Lizzit, Oxygen switching of the epitaxial graphene–metal interaction, ACS Nano **6**, 9551–9558 (2012).

[77] R. Larciprete, P. Lacovig, S. Gardonio, A. Baraldi, and S. Lizzit, Atomic oxygen on graphite: Chemical characterization and thermal reduction, J. Phys. Chem. C **116**, 9900–9908 (2012).

[78] S. Kaciulis, A. Mezzi, P. Calvani, and D.M. Trucchi, Electron spectroscopy of the main allotropes of carbon, Surf. Interface Anal. **46**, 966–969 (2014).

[79] H. Estrade-Szwarckopf, XPS photoemission in carbonaceous materials: A "defect" peak beside the graphitic asymmetric peak, Carbon **42**, 1713–1721 (2004).

[80] D.Q. Yang and E. Sacher, Carbon 1s X-ray photoemission line shape analysis of highly oriented pyrolytic graphite: The influence of structural damage on peak asymmetry, Langmuir **22**, 860–862 (2006).

[81] J.E. Houston, D.E. Ramaker, J.W. Rogers Jr., R.R. Rye, and F.L. Hutson, Dynamic core-hole screening effects in the C-KVV Auger line shape of graphite, Phys. Rev. Lett. **56**, 1302–1304 (1986).

[82] P.I. Belobrov, L.A. Bursill, K.I. Maslakov, and A.P. Dementjev, Electron spectroscopy of nanodiamond surface states, Appl. Surf. Sci. **215**, 169–177 (2003).

[83] E. Perfetto, M. Cini, S. Ugenti, P. Castrucci, M. Scarselli, M. De Crescenzi, F. Rosei, and M.A. El Khakani, Electronic correlations in graphite and carbon nanotubes from Auger spectroscopy, Phys. Rev. B **76**, 233408 (2007).

[84] E. Perfetto, M. Cini, S. Ugenti, P. Castrucci, M. Scarselli, M. De Crescenzi, F. Rosei, and M.A. Khakani, Experimental and theoretical study of electronic correlations in carbon nanotubes and graphite from Auger spectroscopy, J. Phys. Conf. Ser. **100**, 052082 (2008).

[85] L. Nobili, L. Magagnin, R. Bernasconi, F. Livolsi, L. Pedrazzetti, A. Lucotti, S.K. Balijepalli, A. Mezzi, S. Kaciulis, and R. Montanari, Investigation of graphene layers on electrodeposited polycrystalline metals, Surf. Interface Anal. **48**, 456–460 (2016).

[86] L. Pedrazzetti, L. Nobili, L. Magagnin, R. Bernasconi, A. Lucotti, P. Soltani, A. Mezzi, and S. Kaciulis, Growth and characterization of ultrathin carbon films on electrodeposited Cu and Ni, Surf. Interface Anal. **49**, 1088–1094 (2017).

[87] S. Kaciulis, A. Mezzi, P. Soltani, T. de Caro, H. Xia, Y.L. Wang, T. Zhai, and M. Lavorgna, Reduction of graphene oxide by UHV annealing, Surf. Interface Anal. **50**, 1089–1093 (2018).

[88] G.C. Lama, C. Santillo, F. Recupido, J. Liu, L. Verdolotti, R. Marzella, T. Polichetti, S. Kaciulis, and M. Lavorgna, Autoclave-mediated reduction of graphene oxide for enhanced conductive films, Appl. Surf. Sci. **657**, 159741 (2024).

[89] S. Kaciulis, A. Mezzi, P. Soltani, R. Pizzoferrato, E. Ciotta, and P. Prosposito, Graphene quantum dots obtained by unfolding fullerene, Thin Solid Films **673**, 19–25 (2019).

[90] E. Ciotta, S. Paoloni, M. Richetta, P. Prosposito, P. Tagliatesta, C. Lorecchio, I. Venditti, I. Fratoddi, S. Casciardi, and R. Pizzoferrato, Sensitivity to heavy-metal ions of unfolded fullerene quantum dots, Sensors **17**, 2614 (2017).

[91] S. Kaciulis, A. Mezzi, S.K. Balijepalli, M. Lavorgna, and H.S. Xia, Electron spectroscopy of rubber and resin-based composites containing 2D carbon, Thin Solid Films **581**, 80–85 (2015).

[92] A. Jagminas, S. Kaciulis, V. Klimas, A. Reza, S. Mickevicius, and P. Soltani, Fabrication of graphene-alumina heterostructured films with nanotube morphology, J. Phys. Chem. C **120**, 9490–9497 (2016).

[93] Y.-L. Wang, M. Stanzione, H. Xia, G. Buonocore, E. Fortunati, S. Kaciulis, and M. Lavorgna, Effect of mercapto-silanes on the functional properties of highly amorphous vinyl alcohol composites with reduced graphene oxide and cellulose nanocrystals, Composites Sci. Technol. **200**, 108458 (2020).

[94] M. Chougan, F.R. Lamastra, D. Caschera, S. Kaciulis, E. Bolli, C. Mazzuca, S.H. Ghaffar, M.J. Al-Kheetan, G. Montesperelli, and A. Bianco, Cementitious nanocomposites engineered with high-oxidized graphene oxide: Spotting the nano to macro correlation, Ceram. Int. **49**, 964–973 (2023).

[95] M. Chougan, F.R. Lamastra, E. Bolli, D. Caschera, S. Kaciulis, C. Mazzuca, G. Montesperelli, S.H. Ghaffar, M.J. Al-Kheetan, and A. Bianco, Extra-low dosage graphene oxide cementitious nanocomposites: A nano-to macroscale approach, Nanomaterials **11**, 3278 (2021).

[96] N. Yan, G. Buonocore, M. Lavorgna, S. Kaciulis, S.K. Balijepalli, Y. Zhan, H. Xia, and L. Ambrosio, The role of reduced graphene oxide on chemical, mechanical and barrier properties of natural rubber composites, Composites Sci. Technol. **102**, 74–81 (2014).

[97] C. Santillo, Y. Wang, G. Buonocore, G. Gentile, L. Verdolotti, S. Kaciulis, H. Xia, and M. Lavorgna, Hybrid graphenene oxide/cellulose nanofillers to enhance mechanical and barrier properties of chitosan-based composites, Front. Chem. **10**, 926364 (2022).

[98] T. Zhai, L. Verdolotti, S. Kaciulis, P. Cerruti, G. Gentile, H. Xia, M. Stanzione, G. Buonocore, and M. Lavorgna. High piezo-resistive performances of anisotropic composites realized by embedding rGO-based chitosan aerogels into open cell polyurethane foams, Nanoscale **11**, 8835–8844 (2019).

ANGLIES ALOTROPŲ PAVIRŠIAUS ANALIZĖ

S. Kačiulis

Nanostruktūrinių medžiagų tyrimų institutas, Monterotondo Scalo (RM), Italija

Santrauka

Anglies spektroskopija yra labai svarbi kietųjų kūnų paviršiaus analizėje, nes anglies kiekis nusako paviršiaus užterštumo laipsnį. Anglis, kaip teršalas iš oro aplinkos, yra praktiškai randama ant bet kokio kietojo kūno, o C 1s fotoelektroninis spektras dažnai naudojamas elektronų ryšio energijos skalės kalibravimui. Be to, per pastaruosius du dešimtmečius buvo sukurtos ir intensyviai tyrinėtos naujos dvimatės anglies medžiagos: grafenas, fulerenai, nanovamzdeliai bei nanosienelės, kvantiniai taškai ir kt. Didėjant amorfinės anglies (a-C) praktiniam pritaikymui, pvz., deimantinės anglies (DLC), anglies kvantinių taškų (CQDs) ir kt., būtinas šių medžiagų charakterizavimas.

Ši trumpa apžvalga skirta naujų anglimi pagrįstų medžiagų analizei, naudojant paviršiui jautrius metodus: Rentgeno spindulių fotoelektroninę spektroskopiją (XPS) ir Ožė elektroninę spektroskopiją (AES). XPS ir AES technikų derinys leidžia tyrinėti elektronų hibridizaciją anglies medžiagose, t. y. leidžia nustatyti sp^2/sp^3 konfigūracijų santykį, kuris apibrėžia pagrindines jų mechanines, elektrines ir optines savybes. Papildomai buvo pademonstruota, kad toks pat eksperimentinis požiūris gali būti sėkmingai taikomas trimatėms kompozicinėms medžiagoms su dvimate anglimi, pvz., su grafenu arba nanovamzdeliais.